

Analysis, Design, and Simulation of an Axially-partitioned Dielectric-loaded Bi-frequency MILO

Arjun Kumar^{#,*}, Prabhakar Tripathi[#], Smrity Dwivedi[#], and P.K. Jain^{#, @}

[#]Department of Electronics Engineering, Indian Institute of Technology (BHU) Varanasi - 221 005, India

[@]National Institute of Technology Patna - 800 005, India

*E-mail: arjunker.rs.ece15@itbhu.ac.in

ABSTRACT

In this paper, a bi-frequency magnetically insulated line oscillator (MILO) was proposed and designed. The bi-frequency MILO proposed has two axially partitioned slow-wave interaction structures (SWS) and the second SWS is dielectric-loaded to create the frequency shift in the resonant frequency. The conventional MILO device design methodology was followed along with two SWSs separated by a segregation cavity. The dispersion relation of the dielectric-loaded SWS was calculated using an equivalent circuit approach. Furthermore, the cold analysis was carried out to find the energy stored in the different SWSs to validate the device oscillation frequency. The beam wave interaction behaviour and device RF output performance were investigated through 3D PIC (Particle-in-cell) simulation for typical diode voltage of 550 kV, and current 48 kA, respectively. Simulation results illustrate that the proposed MILO generates RF peak power of ~3.5 GW at frequencies 3.62 GHz and 3.72 GHz. The conversion efficiency of the device was ~13.25%.

Keywords: Bi-frequency; Dielectric loading; High power microwaves; MILO; Slow-wave structure

1. INTRODUCTION

In the past few decades, multi-frequency high power microwave (HPM) sources have become significant due to their potential application in the HPM systems¹. Different HPM sources, like transit time oscillator (TTO), relativistic backward wave oscillator (RBWO), and MILO, have been developed to generate bi-frequency RF²⁻⁴. Among these MILO attracts the researcher due to its self-insulation, compact, and lightweight features⁵.

MILO can be used to generate bi-frequency RF power either in two different bands (i.e., also known as dual-band) or in a single band. The dual-band devices can be designed using the combination of two different/same device designing concepts in a single device structure. The reported dual-band devices use two different concepts such as coaxial TTO-MILO, MILO-MILO, and Vircator-MILO⁶⁻⁸. The concept of two different slow-wave structures in a single MILO device has been reported by J-C Ju⁶, *et al.*, where RF can be generated at two different frequencies in L-band (1.72 GHz) and Ku-band (14.6 GHz) with 12.8% conversion efficiency were achieved through simulation. Zhang⁷, *et al.* experimentally reported a VCO-MILO device to generate three frequencies. Two frequencies are generated in S-band (2.1 and 3.8 GHz) while the third in the C-band (4.1 GHz) with an overall efficiency of ~13.44%. Xiao⁸, *et al.* reported a coaxial TTO-MILO and simulated RF power in three frequencies in three-bands with

an overall efficiency of 25.4% has been reported. The main drawback of these designs is the use of separate extraction sections which not only enhances design complexity but causes additional RF losses and reduces device efficiency.

In single-band, bi-frequency devices can generate microwave power at two different frequencies. The device can be designed in two different ways to generate bi-frequency in a single-band which is either varying the interaction structure azimuthally or varying the interaction structure axially. Chen³, *et al.* reported an experimental azimuthally partitioned bi-frequency MILO in which 620 MW power has been achieved at two frequencies with a frequency difference of 250 MHz. Though overall efficiency was found very low ~ 4.3%. Also, the device had a problem with RF power extraction because of its distribution over two asymmetric modes.

To overcome such problems, a novel bi-frequency single-band MILO with axially partitioned SWS is proposed in this paper. In this configuration, two interaction structures separated with a segregation cavity is proposed to be used. The second interaction structure (i.e., SWS2) is partially filled with the dielectric material (i.e., fused quartz) has a relative dielectric constant of 3.8, and dielectric strength lies between the $2.5 \times 10^7 - 4 \times 10^7$ kV/m. The typical Fused Quartz dielectric material has a very low loss tangent (about at 3 GHz) and can be used up to a temperature range of 950-1300 °C. The SWS2 is occupied with a low loss dielectric which shifts the oscillation frequency maintaining an efficient beam-wave interaction process⁹. The function of the dielectric material is to increase the capacitance of the cavity. As we are using low loss

dielectric material, the quality factor ($Q_{\text{dielectric material}} = 1 / \tan \delta$) of the cavity increases, which helps in efficient beam-wave interaction. Here, the proposed device oscillates at two frequencies in the same symmetric mode (i.e., TM_{100} mode) which alleviates the problem faced with the azimuthally partitioned bi-frequency MILO.

2. DEVICE DESIGN METHODOLOGY

The schematic diagram of the bi-frequency MILO is given in Fig. 1. The device mainly consists of a choke section, extractor section along two slow-wave interaction structure sections (SWS_1 and SWS_2), which are separated by a segregation cavity. Here, the SWS_2 dimension is the same as the SWS_1 except it is now partially filled with a low loss dielectric material. The dielectric thickness is taken as \sim one-fourth of the cavity depth⁹. Here, the dielectric is chosen in such a way that it only changes the fundamental mode frequency associated with SWS_2 . The segregation cavity is primarily used for eliminating the lower frequency microwaves leakage (i.e., the resonating frequency associated with the SWS_2) to the higher frequency (i.e., the resonating frequency associated with the SWS_1) in the device⁶. An explosive emissive cathode is selected for the generation of the electron.

An axially-partitioned SWS MILO is designed following the approach of the conventional MILO^{10,11}. The interference between the two resonant frequencies which is generated due to the use of two different SWS is avoided by a proper length of the segregation cavity. The segregation cavity length of 1.5 times of the disc periodicity (L) is sufficient. The device's electrical parameter and dimension are tabulated in Table 1.

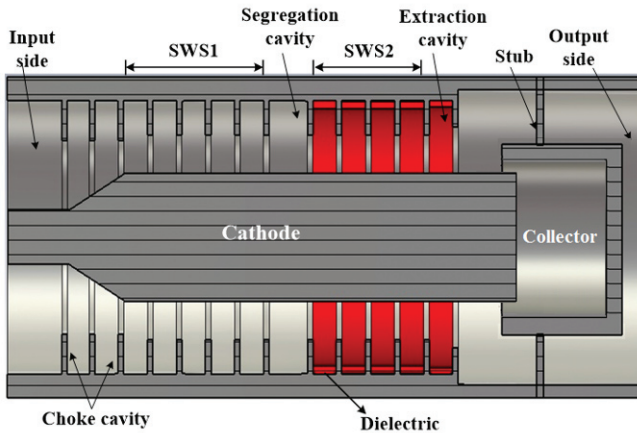


Figure 1. The schematic diagram of proposed bi-frequency MILO.

3. ANALYSIS

The periodic disc-loaded coaxial structure which is partially filled with the dielectric material of low loss is analysed with the help of the equivalent circuit approach. A single-cavity of the SWS and its equivalent circuit is shown in Fig. 2. The equivalent circuit inductance (L_e) and equivalent capacitance (C_e), which are typically used for calculating the frequency of the fundamental mode of the individual cavity.

Table 1. Design specification of the axial partition dielectric-loaded bi-frequency MILO

Parameters	Values
Current	48 kA
Voltage	550 kV
Anode radius (R_{ao})	64.0 mm
Cathode radius (R_c)	30.0 mm
Choke disc radius (R_{ch})	45.0 mm
SWS disc radius (R_{ai})	48 mm
Extractor disc radius (R_{ext})	54.0 mm
Dielectric thickness (d_{th})	4.0 mm
Disc periodicity (L)	16.0 mm
Disc thickness (T)	3.0 mm

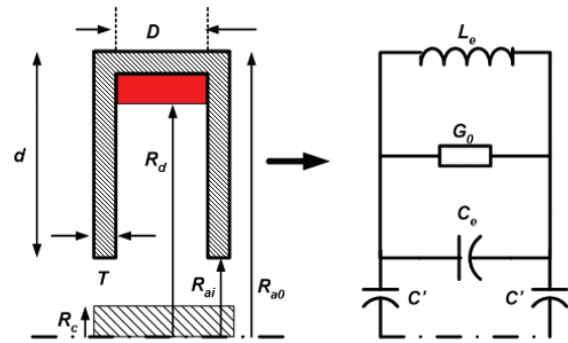


Figure 2. Single dielectric-loaded cavity and its equivalent circuit.

In SWS, each resonant cavity is coupled to the adjacent cavity through the capacitive coupling. The resonance condition of the structure can also be evaluated by calculating the relationship between the resonant frequency in the adjacent cavity and the phase difference corresponding to them, also known as the dispersion relation.

For the axial-partition dielectric-loaded bi-frequency MILO, the mode for operation is π -mode. At this mode, the phase velocity approximately equal to the electrons drift velocity and the group velocity becomes very close to zero. The electromagnetic characterisation of the disc loaded coaxial structure is performed to calculate the energy associated with different frequencies. It also provides information regarding the external quality factor (Q_{ext}) of the structure.

3.1 Equivalent Inductance and Capacitance of the Cavity

The fundamental mode low loss dielectric cavity equivalent LC circuit can be shown in Fig. 2.

The equivalent inductance of the dielectric-loaded cavity can be given as¹²:

$$L_e = \frac{\mu_0 dD}{4\pi R_{ao}} \quad (1)$$

Its equivalent capacitance can be defined as⁹:

$$C_e = 2\varepsilon_0 R_{ai} \ln\left(\frac{D+2T}{D}\right) + \frac{2\pi}{3dD} \left[\varepsilon_0 (3R_{a0}R_d^2 - 3R_{a0}R_{ai}^2 - 2R_d^3 + 2R_{ai}^3) + \varepsilon_r (R_{a0}^3 + 2R_d^3 - 3R_{a0}R_d^2) \right] \quad (2)$$

where ε_0 and μ_0 are the permittivity and permeability of the vacuum. R_{a0} , R_{ai} , D , T , d , R_c , and R_d are the other circuit parameters. The coupling capacitance which couples the electric field with the consecutive cavity can be calculated as⁹:

$$C' = \frac{2\pi\varepsilon_0 T}{\ln(R_{ai}/R_c)} + 8\varepsilon_0 [D + (R_{ai} - 2(R_{ai} - R_c)/\pi) \times \ln(\frac{\pi D + 2(R_{ai} - R_c)}{2(R_{ai} - R_c)})] \quad (3)$$

The resonance frequency (ω_{0k}) of the circuit formed by the coaxial disc loading can be given as:

$$\omega_{0k} = \omega_0 / \sqrt{1 + \frac{C'}{C_e} \left(\frac{1}{1 - \cos(\beta_0 L)} \right)} \quad (4)$$

where, $\omega_0 = 1/\sqrt{L_e C_e}$ β_0 is the axial phase constant, the dielectric constant $\varepsilon_r = 1$ for SWS₁ and SWS₂ typically taken as $\varepsilon_r = 3.9$.

Using expressions (1) to (4), the structure dispersion is obtained and plotted in Fig. 3. Here, the beam wave interaction region can be identified with the help of beam-mode and light-velocity lines as $\omega = \beta_0 v_e$, and $\omega = \beta_0 c$, respectively. Here, ω is the angular frequency, c is light velocity, and v_e is the electrons drift velocity⁵.

3.2 Cold EM Characterisation of Cavity Structures

Cold electromagnetic (EM) characterisation of the disc-loaded coaxial structure gives information about its resonant frequencies, supported modes, and EM fields excitation in absence of the external electrons. A 550 kV DC pulse voltage was applied between anode and cathode with matched boundary conditions. After applying the TEM wave at one end and waiting for 50 ns, the electromagnetic energy stored inside the cavity can be calculated by volume integration of the electromagnetic energy density¹³. The total stored energy is the sum of electric field energy and magnetic field energy.

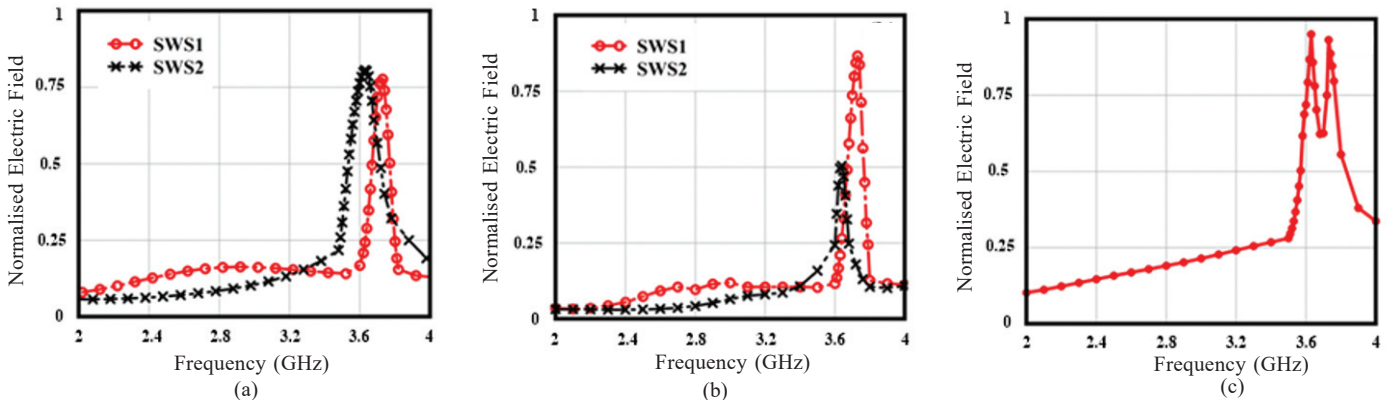


Figure 4. (a) Normalised electric field (b) Normalised magnetic field and (c) Normalised energy stored inside the SWS cavities at different frequencies.

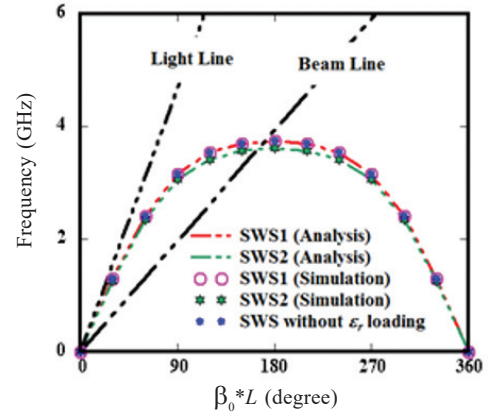


Figure 3. Dispersion diagram of the axial-partitioned dielectric-loaded bi-frequency MILO.

Figures 4(a), 4(b), and 4(c) show the normalised electric field, normalised magnetic field, and normalised energy, respectively. From Figs. 4(a) and 4(b), it can be clearly observed that the electric field plays a more significant role in beam wave RF interaction as compared to the magnetic field. The total energy is mainly distributed in two frequencies i.e., 3.62 GHz and 3.72 GHz which is almost equal and it can be clearly noticed from these figures.

4. DEVICE SIMULATION

To verify the design parameter (i.e., listed in Table-1), the dispersion relation is obtained from the CST eigenmode solver. Further, the proposed bi-frequency MILO is simulated using particle-in-cell code “CST Particle Studio” with the typically taken beam parameter (i.e., 550 kV beam voltage with explosive electrons emission condition). In addition, the parametric study is also performed to optimise the dielectric constant and thickness of the loading material.

4.1 Eigenmode Simulation

In this subsection, the structural design is validated with the help of the cold test (i.e., without electron beam) simulation study. Here, we calculate the phase difference between the consecutive discs corresponding to the operating frequencies (dispersion relation) for two different SWS. Figure 3 shows the dispersion relation of the two SWS sections. The observation

from Fig. 3 shows that the π -mode operating frequency is around 3.62 GHz and 3.72 GHz, which corroborates our design. Through the simulation, it is noticed structure the resonance frequencies can be controlled either by changing the dielectric constant (ϵ_r) or its thickness. The maximum frequency difference is limited by the phase velocity of resonating modes supported by the SWS.

4.2 PIC Simulation

In this subsection, the behaviour of beam wave interaction and RF output performance of the proposed device in terms of power, efficiency, etc. is investigated by performing the hot test (i.e., in the presence of electron beam) simulation study.

For electron beam generation with explosive emission conditions the high voltage DC pulse is given between the anode and cathode¹⁴. DC voltage pulse with 5 ns rise time and 65 ns of hold time, a single pulse of 550 kV is applied at the input port. After achieving the self-magnetic insulation; the electron sheath restricts between the cathode and the tips of the disc along the axial direction⁵. This magnetically insulated electron sheath incites noise within the cavities and generates oscillations. Thus, the energy is stored within the cavities in terms of the standing wave and this standing wave converted into a travelling wave by the extractor cavity⁵.

Beam-wave interaction process at different time instants with (a) magnetic insulation phase, and (b) nonlinear phase are shown in Fig. 5. In the nonlinear phase; the spoke-like cloud formation between the consecutive discs cavities is formed inside the device which confirms optimum beam wave interaction. Further, inside the device, the temporal RF signal growth is recorded at the output waveguide port. Figure 6 shows the applied input DC voltage pulse and generated RF signal. It can be seen that after 25 ns RF signal is showing a ripple-like behaviour. This ripple behaviour of RF signal is because of the synthesis of two frequencies and considered as beating phenomenon^{2,3}.

Similar RF growth behaviour has been observed in other reported bi-frequency HPM devices (RBWO², MILO³). The separation of the two frequencies is very difficult. The FFT of the output RF signal gives the frequency spectrum which is shown in the above Fig. 7.

It can be clearly observed here that the designed device is radiating RF signals at 3.62 GHz and 3.72 GHz frequencies. The normalised amplitude difference between the two frequencies is 4.3% which indicates that almost equal RF power is distributed between them. The generated RF power is shown in Fig. 8 where RF peak power of ~3.5 GW and average power of ~1.75 GW can be observed. The energy associated with the RF signal calculated with the time integration of average power and found as ~75 J. The overall efficiency with peak power achieved by the proposed MILO is ~13.25% and with the average power ~6.62%.

4.3 Parametric Study

A study of the RF behaviour of the MILO device with different dielectric loading has been performed with the device simulation for the different dielectric constants (ϵ_r) and plotted in Fig. 9.

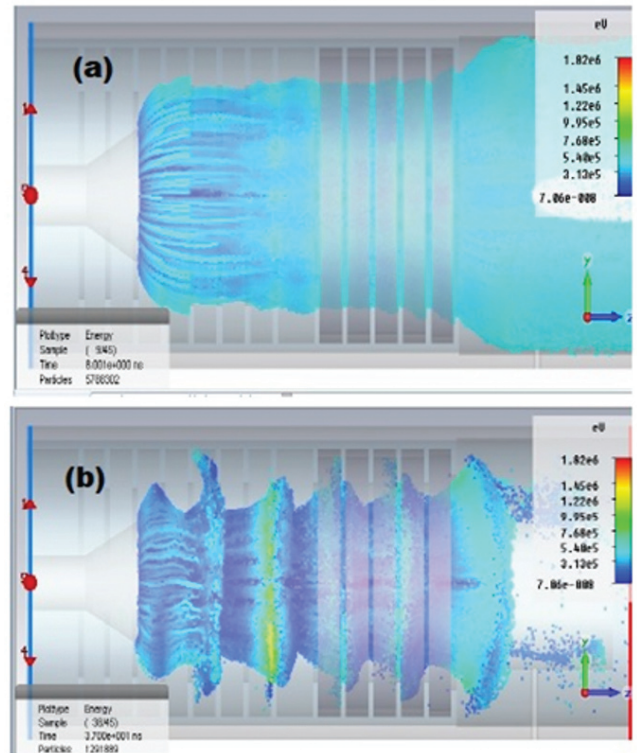


Figure 5. Beam wave interaction at different positions inside the device (a) Magnetic insulation phase (b) Non-linear phase.

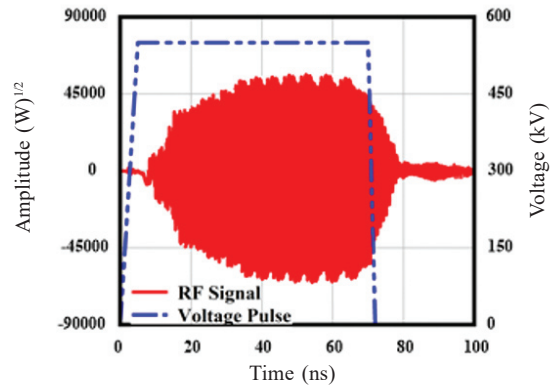


Figure 6. Input DC voltage pulse and RF signal growth at the extraction section of the proposed MILO.

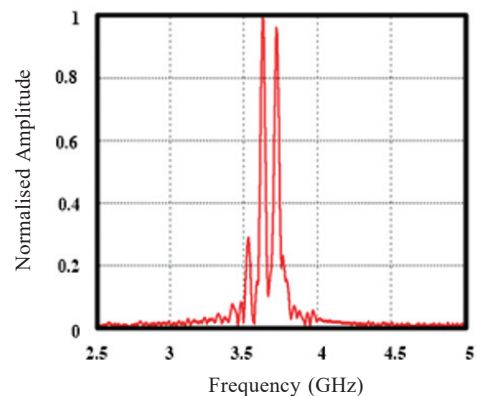


Figure 7. RF output frequency spectrum (3.62 GHz and 3.72 GHz).

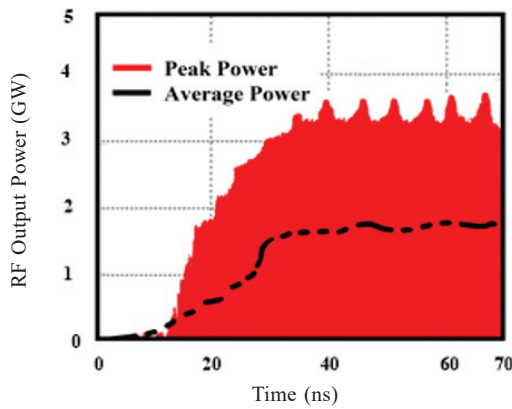


Figure 8. RF output peak and average powers of the designed bi-frequency MILO.

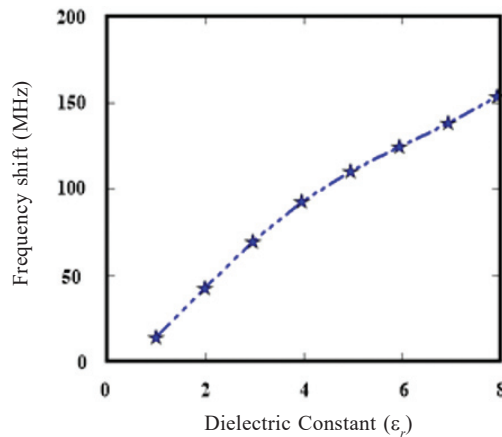


Figure 9. Frequency shift in the π -point of the proposed MILO due to change in the dielectric loading.

The effect of the dielectric constant on the π -mode frequency shifting between two operating frequencies (i.e., f_1 - f_2) of the device that as the dielectric loading increases, the frequency difference is also increased. Similarly, Fig. 10 shows the effect of dielectric loading on the device RF growth and efficiency. It is found from Fig. 10, that maximum RF power and efficiency can be obtained at an optimised dielectric loading. For a typical selected case, it is found as $\epsilon_r = 4$.

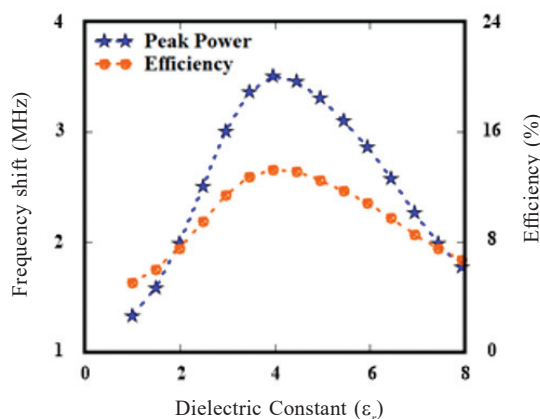


Figure 10. Effect of dielectric loading on proposed MILO RF peak power output and device efficiency.

5. CONCLUSION

In this paper, the study of axially-partitioned dielectric-loaded bi-frequency MILO has been proposed and analysed using equivalent circuit analysis. The device design and performance is validated through simulation studies. The structural design analysis, eigenmode simulation is performed. The resonating frequency of the device interaction structure is calculated using the dispersion curve through analysis and eigenmode simulation. In addition, the cold analysis is carried out to find out the energy stored in the two SWSs structure. Finally, the beam-wave interaction and total performance of the MILO device proposed here is investigated through PIC simulation. RF peak power of ~ 3.5 GW and average power of ~ 1.75 GW is obtained at two frequencies, 3.62 GHz and 3.72 GHz. The designed device conversion efficiency achieved is $\sim 13.25\%$ and $\sim 6.62\%$, respectively.

REFERENCES

1. Barker, R. J.; & Schamiloglu, E. High-power microwave sources and technologies. *IEEE Press*, 2001.
2. Tang, Y.; Meng, L.; Li, H.; Zheng, L.; Wang, B. & Yin, Y. An X-band dual-frequency coaxial relativistic backward-wave oscillator. *IEEE Trans. Plasma Sci.*, 2012, **40**(12), 3552-3559. doi: 10.1109/TPS.2012.2222671
3. Chen, D. B.; Wang, D.; Meng, F. B. & Fan, Z. K. Bifrequency magnetically insulated transmission line oscillator. *IEEE Trans. Plasma Sci.*, 2012, **37**(1), 23-29. doi: 10.1109/TPS.2008.2007731
4. He, J.; Cao, Y.; Zhang, J.; Wang, T. & Ling, J. Design of a dual-frequency high-power microwave generator. *Laser and Particle Beams*, 2011, **29**(4), 479-485. doi: 10.1017/S0263034611000590
5. Dixit, G.; Kumar, A. & Jain, P. K. Design analysis and simulation study of an efficiency enhanced L-band MILO. *Phy. Plasmas*, 2017, **24**(1), p.013113. doi: 10.1063/1.4973929
6. Ju, J. C.; Fan, Y. W.; Shu, T. & Zhong, H. H. Proposal of a gigawatt-class L/Ku dual-band magnetically insulated transmission line oscillator. *Phy. Plasmas*, 2014, **21**(10), 103104. doi: 10.1063/1.4897937
7. Zhang, X.; Li, Y.; Li, Z.; Zhong, H. & Qian, B. Preliminary experimental investigation of a complex dual-band high power microwave source. *Rev. Sci. Inst.*, 2015, **86**(10), 104703. doi: 10.1063/1.4934246
8. Xiao, R.; Sun, J.; Chen, C.; Zhang, Y. & Shao, H. High efficiency annular magnetically insulated line oscillator-transit time oscillator with three separate frequencies in three bands. *J. Applied Physics*, 2009, **106**(3), 033308. doi: 10.1063/1.3190532
9. Fan, Y. W.; Wang, X. Y.; Zhong, H. H. & Zhang, J. D. A dielectric-filled magnetically insulated transmission line oscillator. *Applied Physics Letters*, 2015, **106**(9), 093501. doi: 10.1063/1.4913932
10. Dwivedi, S. & Jain, P. K. Beam-wave interaction

- analysis of a magnetically insulated line oscillator. *Phy. Plasmas*, 2012, **19**(8), 082110.
doi: 10.1063/1.4743023
11. Dwivedi, S. & Jain, P. K. Design expressions for the magnetically insulated line oscillator. *IEEE Trans. Plasma Sci.*, 2013, **41**(5), 1549-1556.
doi: 10.1109/TPS.2013.2256470
 12. Fan, Y.W.; Zhong, H. H.; Shu, T. & Li, Z.Q. Theoretical investigation of the fundamental mode frequency of the magnetically insulated transmission line oscillator. *Phy. Plasmas*, 2008, **15**(12), 123504.
doi: 10.1063/1.3028315
 13. Cousin, R.; Larour, J.; Raymond, P.; Wey, J.; Gouard, P. & Durand, A. J. Theoretical and experimental behavior of a compact magnetically insulated line oscillator electromagnetic structure. *Rev. of sci. inst.*, 2005, **76**(12), 124701-124708.
doi: 10.1063/1.2141004
 14. Mahto, M. & Jain, P. K. Parametric study of the reltron oscillators. *Def. Sci. J.*, 2019, **69**(5), 448-452.
doi: 10.14429/dsj.69.14949

CONTRIBUTORS

Mr Arjun Kumar received the BTech in ECE from Biju Patnaik University of Technology, Odisha, India, in 2013. Currently, he is a research scholar in Electronics Engineering with IIT (BHU), Varanasi, India. His current research interests include computational electromagnetics and HPM Sources.

He contributed to the research work in conceptualisation, modelling, simulation, result analysis, and preparing the initial draft of the manuscript.

Dr Prabhakar Tripathi received his BTech in 2009 and MTech in 2011 from U.P.T.U, Lucknow, India and Graphic Era University, Dehradun, Uttarakhand, India, respectively. Presently, he is a research scholar in the Electronics Department of IIT (BHU), Varanasi, India. He received the Visvesvaraya PhD Scheme for the financial support of his research work. His area of research interests includes HPM sources, Electromagnetic analysis, and Slow-wave structures.

His contributions to the current research work include conceptualisation, review, and editing of the manuscript.

Dr Smrity Dwivedi received the BTech in 2005 from U.P.T.U, Lucknow, India, in ECE and the PhD in 2013 from IIT (BHU), Varanasi, India. After that, she joined as Assistant Professor in the Electronics Department of IIT Varanasi in 2017. Her area of research includes modelling, simulation, and design of HPM sources.

She contributed to the research with her valuable supervision. She helped in the conceptualisation, review, and editing of the research study.

Dr Pradip Kumar Jain received his BTech, MTech and PhD in 1979, 1981, and 1988, respectively from IIT (BHU), Varanasi, India. He joined as a Lecturer, in 1981 in the Electronics Department of IIT (BHU) Varanasi and became a Professor in 2001. Currently, he is the Director of NIT, Patna, India. His area of expertise in the research are modelling, simulation, design, and development of different microwave/millimeter-wave high-power devices and components such as MILO, Reltron, Gyro-TWT, Gyrotron, Mode-converter. His research interest also includes metamaterial-based applications, plasmonics, and through-wall imaging.

He contributed to the research with his valuable supervision. He helped in the conceptualisation, review, and editing of the research study.